



Available online at www.sciencedirect.com

ScienceDirect

Geochimica et Cosmochimica Acta 290 (2020) 27-40

Geochimica et Cosmochimica Acta

www.elsevier.com/locate/gca

First-principles computation of diffusional Mg isotope fractionation in silicate melts

Haiyang Luo a,*, Bijaya B. Karki a,b,c, Dipta B. Ghosh b, Huiming Bao a

Department of Geology & Geophysics, Louisiana State University, Baton Rouge, LA 70803, USA
 School of Electrical Engineering and Computer Science, Louisiana State University, USA
 Center for Computation and Technology, Louisiana State University, USA

Received 3 December 2019; accepted in revised form 26 August 2020; Available online 4 September 2020

Abstract

Diffusional isotope fractionation occurs in geochemical processes (such as magma mixing, bubble growth, and crystal growth), even at magmatic temperatures. Isotopic mass dependence of diffusion is commonly expressed as $\frac{D_i}{D_i} = \left(\frac{m_j}{m_i}\right)^{\beta}$, where D_i and D_i are diffusion coefficients of two isotopes whose masses are m_i and m_i . How the dimensionless empirical parameter β depends on temperature, pressure, and composition remains poorly constrained. Here, we conducted a series of first-principles molecular dynamics simulations to evaluate the β factor of Mg isotopes in MgSiO₃ and Mg₂SiO₄ melts using pseudo-isotope method. In particular, we considered interactions between Mg isotopes by simultaneously putting pseudo-mass and normalmass Mg atoms in a simulation supercell. The calculated β for Mg isotopes decreases linearly with decreasing temperature at zero pressure, from 0.158 ± 0.004 at 4000 K to 0.121 ± 0.017 at 2200 K for MgSiO₃ melt and from 0.150 ± 0.004 at 4000 K to 0.101 ± 0.012 at 2200 K for Mg₂SiO₄ melt. Moreover, our simulations of compressed Mg₂SiO₄ melt along the 3000 K isotherm show that the β value decreases linearly from 0.130 ± 0.006 at 0 GPa to 0.060 ± 0.011 at 17 GPa. Based on our diffusivity results, the empirically established positive correlation between β and solvent-normalized diffusivity (D_i/D_{Si}) seems to be applicable only at constant temperatures or in narrow temperature ranges. Analysis of atomistic mechanisms suggests that the calculated β values are inversely correlated with force constants of Mg at a given temperature or pressure. Good agreement between our first principles results with available experimental data suggests that interactions between isotopes of major elements must be considered in calculating β for major elements in silicate melts. Also, we discuss diffusion-controlled crystal growth by considering our calculated β values. © 2020 Elsevier Ltd. All rights reserved.

Keywords: Isotope fractionation; Diffusivity; First-principles computation; Silicate melts

1. INTRODUCTION

Many geological processes have been taking place in diverse magmatic systems, e.g. crystal and bubble growth from silicate melts, melt-rock interaction, and magma recharge and mixing. An important geochemical finger-print left by these igneous processes is stable isotope

composition of elements. Owing to improved isotope measurement techniques, variations in stable isotope compositions between minerals and within a mineral can be detected. Both equilibrium and kinetic effects may fractionate isotopes according to their mass differences. The degree of equilibrium isotope fractionation generally decreases with increasing temperature, resulting in smaller fractionation in magmatic systems than at surface temperatures (Bigeleisen and Mayer, 1947; Urey, 1947). Non-equilibrium isotope fractionation processes depend

^{*} Corresponding author.

E-mail address: hluo5@lsu.edu (H. Luo).

on kinetic isotope effects and reaction progress. Apparent isotope fractionation can be large even at magmatic temperatures, e.g. heavy isotope enrichment in residues during evaporation. (e.g. Clayton et al., 1988; Davis et al., 1990; Wang, 1994; Knight et al., 2009; Richter et al., 2009a, 2002, 2007; Zhang et al., 2014; Mendybaev et al., 2017). Another process that may lead to large isotope fractionation at magmatic temperatures is diffusion, including thermal diffusion (e.g. Richter et al., 2008, 2009a, 2014; Huang et al., 2009, 2010; Dominguez et al., 2011; Lacks et al., 2012: Fortin et al., 2019) and chemical diffusion (e.g. Richter et al., 1999, 2003, 2008, 2009a, 2009b; Teng et al., 2006; Watkins et al., 2009, 2011, 2014; Dauphas et al., 2010; Teng et al., 2011; Chopra et al., 2012; Sio et al., 2013, 2018; Oeser et al., 2015; Fortin et al., 2017; Holycross et al., 2018; Wu et al., 2018).

Chemical diffusion may cause significant isotope fractionation in both silicate minerals and melts. A comprehensive review of the theories of isotope separation by diffusion in silicate minerals was given by Van Orman and Krawczynski (2015). Diffusive separation of isotopes in silicate melts was found to play important role in three common geochemical processes, magma mixing (Richter et al., 1999; Chopra et al., 2012), crystal growth (Watson and Müller, 2009; Antonelli et al., 2019), and bubble growth (Fortin et al., 2017; Watson, 2017). To interpret measured isotope data and recover thermal evolutions and time scales of these processes, we must first determine the magnitude of diffusional isotope fractionation and its possible relationships with temperature, pressure, and composition.

Isotopic mass dependency of diffusion is commonly expressed as (Richter et al., 1999):

$$\frac{D_i}{D_j} = \left(\frac{m_j}{m_i}\right)^{\beta} \tag{1}$$

where D_i and D_j are diffusion coefficients of two isotopes whose masses are m_i and m_j and β is a dimensionless empirical parameter. For an ideal monatomic gas, $\beta = 0.5$, as predicted by kinetic theory of gases (Chapman, 1970). However, it has been difficult to predict diffusional isotope fractionation factors in liquids because diffusing units interact constantly with their nearest neighbors, making it difficult to identify the true diffusing species. As a result, the β factor based on isotopic mass is expected to be lower than 0.5 and be dependent on variables, such as temperature, pressure, and chemical composition.

Several experiments have been conducted to calibrate mass-dependent diffusivities of isotopes in silicate melts and the β factors for different elements (Li, Mg, S, Cl, Ca, Fe, Ge) were found to range from 0 to 0.22 (Richter et al., 1999, 2003, 2008, 2009b; Fortin et al., 2017, 2019; Watkins et al., 2009; Watkins et al., 2011, 2014; Holycross et al., 2018). Watkins et al. (2011) confirmed compositional effects on β in albite-anorthite and albite-diopside diffusion couple experiments. Goel et al. (2012) studied the pressure dependence of β by performing molecular dynamics (MD) simulations of MgSiO₃ melt from 0 to 50 GPa. In comparison, the temperature dependence of β has so far not been resolved in experiments. A possible

explanation is that the limited range of temperatures explored by experiments is insufficient to reveal the variations of β due to relatively large uncertainties associated with isotope measurement and necessary diffusion profile modeling. First-principles molecular dynamics (FPMD) simulations have provided reliable atomistic insights into the structural and dynamical properties of silicate melts over the entire Earth's mantle conditions (e.g., Stixrude and Karki, 2005; Ghosh and Karki, 2011; Bajgain et al., 2015; Caracas et al., 2019; Solomatova and Caracas, 2019). It is expected that FPMD results may provide reliable constraints on diffusional isotope fractionation parameters, including the effects of temperature, pressure, and composition, as well as those related to atomic mechanisms.

The work of Liu et al. (2018) is so far the only FPMD simulation study on diffusive separation of isotopes in silicate melts. They simulated MgSiO₃ and Mg₂SiO₄ melts at 0 GPa and obtained a β value of 0.272 \pm 0.005 for Mg isotopes in MgSiO₃ melt at 4000 K, and β of $0.184 \pm 0.006, 0.245 \pm 0.007,$ and 0.257 ± 0.012 for Mg isotopes in Mg₂SiO₄ melts at 2300, 3000 and 4000 K, respectively. From the experimental side, Richter et al. (2008) reported $\beta = 0.050 \pm 0.005$, in basalt-rhyolite diffusion couple experiments at 1400 °C and 1 GPa and Watkins et al. (2011) obtained a Mg β factor of 0.100 ± 0.010 in albitediopside diffusion couple experiments at 1450 °C and 8 kbar. Based on classical MD simulations, Goel et al. (2012) calculated a β value of 0.135 ± 0.008 for Mg in MgSiO₃ melt at 4000 K and 0 GPa. The results from diffusion experiments and classical MD simulations are all much smaller than those of Liu et al. (2018). Liu et al. (2018) attributed the discrepancy between experiments and their FPMD simulations to large temperature and compositional differences and they suggested specifically the disparity between classical MD and FPMD simulations is due to different methods used in handling interatomic potentials. All Mg atoms with normal mass were substituted by another set of Mg atoms with same pseudo mass in their simulations (Liu et al., 2018). This full substitution approach does not consider the interaction a heavy isotope of a major element is having with its ambient other lighter isotopes of the major element. Our hypothesis is that the use of the full substitution approach enlarges the difference in diffusion coefficients of isotopes of interest and results in an overestimation of the β value.

In the present study, we replace the full substitution approach with a partial substitution approach, as it better corresponds to a realistic scenario. We examined diffusional Mg isotope fractionation in MgSiO₃ and Mg₂SiO₄ melts at 4000, 3000, 2500, and 2200 K around zero pressure, as well as Mg₂SiO₄ melts at \sim 8 and 17 GPa, at 3000 K. Simulations over wide temperature and pressure ranges allowed us to examine the effects of temperature and pressure on β and to probe into microscopic mechanisms of diffusional isotope effect. The relationship between β and solvent-normalized diffusivities (D_i/D_{Si}) was also examined. A diffusion-controlled crystal growth model (Watson and Müller, 2009) was used to briefly discuss the effects of our calculated β on isotope fractionation between a growing crystal and melt.

2. METHODS

We used first-principles molecular dynamics (FPMD) technique within local density approximation (Ceperley and Alder, 1980) and projector augmented wave method (Blochl, 1994; Kresse and Joubert, 1999) as implemented in the Vienna Ab-initio Simulation Package (Kresse and Furthmüller, 1996). An energy cutoff of 400 eV and the gamma point sampling were used. A canonical ensemble (NVT) with periodic boundary conditions was adopted using a cubic supercell consisting of 16 MgSiO₃ units (16 Mg, total 80 atoms) and 16 Mg₂SiO₄ units (32 Mg, total 112 atoms). The initial structure was melted at 8000 K and then guenched down to 6000, 4000, 3000, 2500, and finally to 2200 K. The Mg₂SiO₄ melt at 3000 K was then compressed to reach two upper mantle pressures, 8.1 and 17 GPa. Further details of these simulations can be found elsewhere (Ghosh and Karki, 2011; Karki, 2010).

To simulate diffusion of Mg isotopes, we use pseudoisotope approach by considering isotope masses $M^* = 1$, 6, 24, 48, 120 g/mol, as was done in Liu et al. (2018). The interactions between Mg isotopes were considered by substituting half (8/16 for MgSiO₃ and 16/32 for Mg₂SiO₄) of the normal Mg ($M^* = 24$) with one type of Mg pseudo-isotopes (e.g. $M^* = 1$) in each simulation. Two simulations of substituting different fractions (6/32, 24/32) of normal Mg in Mg₂SiO₄ melts at 4000 K were also conducted. Two full substitutions (16/16 for MgSiO₃ and 32/32 for Mg₂SiO₄) were tested for comparison with the results of Liu et al. (2018) who used the full substitution approach. This comparison also allowed us to assess the finite size effect because Liu et al. (2018) used larger supercells consisting of 32 MgSiO₃ units and 32 Mg₂SiO₄ units. Finite size effect under half substitution was also checked with 160 atoms (32 MgSiO₃ units) in one simulation at 4000 K. We also explored the influence of the choice of exchange-correlation functional by conducting two simulations with generalized gradient approximation (GGA) pseudopotential in MgSiO₃ and Mg₂SiO₄ melts at 4000 K. In all our simulations, a time step of 1 femtosecond was used. To achieve an acceptable convergence, we ran simulations of Mg₂SiO₄ and MgSiO₃ melts with durations ranging from 50 to 300 picoseconds, and from 150 to 550 picoseconds, respectively (Table 1).

The self-diffusion coefficient D_{α} of species α in melts (which represents a pseudo Mg isotope in our case) can be derived using the Einstein relation (Einstein, 1956):

$$D_{\alpha} = \lim_{t \to \infty} \frac{\left\langle \left| \overrightarrow{r}(t+t_0) - \overrightarrow{r}(t) \right|^2 \right\rangle_{\alpha}}{6t} \tag{2}$$

where $\overrightarrow{r}(t)$ denotes the particle trajectories and $\langle \cdots \rangle_{\alpha}$ represents average mean square displacement (MSD) over time and over all atoms of the species α from different time origins t_0 . Each simulation was divided into 4 blocks after removing the last 30% data due to poor statistics at the end and the standard error (SE) of block-averaged self-diffusion coefficients was calculated. Confidence intervals on D_{α} are reported as \pm 2SE. Given a trade-off between time limit and precision of D_{α} (Bourg and Sposito, 2007; Bourg and Sposito, 2008; Bourg et al.,

2010), we approximated the infinite time limit in Eq. (2) by averaging D_{α} for the first picosecond after a clear diffusive regime is reached as discussed in Section 3.1. β in Eq. (1) for Mg isotopes at each temperature can be derived from the fitted lines in the plot of $ln(D_{24}/D_{\alpha})$ versus $ln(M_{\alpha}/M_{24})$. Confidence intervals on $ln(D_{24}/D_{\alpha})$ were calculated by error propagation. The errors of β were given by the linear fitting.

To analyze the effects of local environment on diffusional Mg isotope fractionation, we examine Mg—O bonding and coordination environments. This requires the calculation of the radial distribution function between Mg and O atoms:

$$g_{AB}(r) = \frac{1}{4\pi\rho_B\gamma^2} \left[\frac{dN_B(r)}{dr} \right] \tag{3}$$

where ρ_B is the number density of O atoms and N_B is the number of O atoms within a sphere of radius of r around a selected atom of type A (which is Mg isotope here). The mean Mg—O bond length is given by a weighted average of all distances covered by the first peak (McQuarrie, 1976):

$$\hat{r}_{AB} = \frac{\int_{0}^{r_{min}} r g_{AB}(r) dr}{\int_{0}^{r_{min}} g_{AB}(r) dr}$$
(4)

where r_{min}^{AB} is the position of the first minimum after the first peak in the $g_{AB}(r)$. Note that the mean Mg—O bond length is somewhat larger than the position of the first peak due to the asymmetry of the peak. The mean atomic coordination of Mg with respect to O can be calculated as

$$C_{AB} = 4\pi \rho_B \int_0^{r_{min}^{AB}} r^2 g_{AB}(r) dr \tag{5}$$

where $A \wedge B$ represent Mg isotope and O, respectively, in our case.

3. RESULTS

3.1. MSD and diffusion coefficients

A typical MSD curve consists of an initial ballistic regime (MSD $\sim t^2$), followed by an intermediate regime, and finally the diffusive regime (MSD $\sim t$) from which the diffusion coefficient is estimated. An example of MSD and corresponding calculated diffusion coefficients of Mg isotopes using Eq. (2) in Mg₂SiO₄ melt at 4000 K is shown in Fig. 1. The MSD-time curves of different pseudoisotopes are clearly separated from each other (Fig. 1a & c). The MSD-time curves of ²⁴Mg are also separated from each other in the diffusive regime, although the differences are much smaller (Fig. 1b & c). Diffusion coefficients of Mg isotopes calculated from the corresponding MSDtime curves at all other conditions in Mg₂SiO₄ and MgSiO₃ melts are shown in Figs. S1 and S2. The residence time of the diffusing atom(s) in the intermediate regime is sensitive to temperature, pressure, and composition. Longer simulations are required to obtain converged diffusion coefficients at decreased temperatures or increased pressures. Owing to a comparatively lower proportion of Si with respect to Mg, the diffusive regime is reached faster in Mg₂SiO₄ melts than

Table 1 Diffusivities of Mg isotopes (with mass M_z), Si and O, Mg—O bond length, coordination number, and bond break rate in Mg₂SiO₄ and MgSiO₃ melts at different temperatures around zero pressure (± 1 GPa) under half substitution of ²⁴Mg. Noted that Mg—O bond break rate is based on ²⁴Mg data. Diffusivity data with other substitution ratios is reported in Table S1.

	$T(\mathbf{K})$	Time (ps)	M_{α} (g/mol)	$D_{\alpha} (10^{-9} \text{ m}^2/\text{s})$	$D_{Mg}^{24} (10^{-9} \text{ m}^2/\text{s})$	$D_{Si} (10^{-9} \text{ m}^2/\text{s})$	$D_O (10^{-9} \text{ m}^2/\text{s})$	$d_{Mg\text{-}O}\left(\mathring{\mathbf{A}}\right)$	Z_{Mg-O}	$1/\tau_{Mg-O}~({\rm ps}^{-1})$
Mg ₂ SiO ₄	2200	300	1	4.42 ± 0.06	3.26 ± 0.14	0.68 ± 0.04	0.94 ± 0.02	2.124	4.96	2.49
	2200	300	6	3.39 ± 0.16	2.89 ± 0.19	0.74 ± 0.06	0.89 ± 0.04	2.125	4.99	2.48
	2200	300	48	2.31 ± 0.09	2.57 ± 0.14	0.55 ± 0.02	0.78 ± 0.01	2.122	4.96	2.48
	2200	300	120	1.82 ± 0.12	2.17 ± 0.11	0.50 ± 0.01	0.73 ± 0.01	2.125	4.99	2.48
	2500	250	1	7.82 ± 0.49	5.74 ± 0.07	1.39 ± 0.09	1.72 ± 0.05	2.127	4.84	2.79
	2500	250	6	5.99 ± 0.28	4.86 ± 0.17	1.16 ± 0.03	1.46 ± 0.02	2.126	4.83	2.76
	2500	250	48	3.94 ± 0.30	4.35 ± 0.56	1.06 ± 0.08	1.54 ± 0.02	2.126	4.84	2.80
	2500	250	120	3.23 ± 0.09	3.97 ± 0.22	1.00 ± 0.03	1.31 ± 0.00	2.127	4.87	2.78
	3000	100	1	15.7 ± 0.9	11.6 ± 1.0	3.34 ± 0.18	4.77 ± 0.06	2.131	4.71	3.29
	3000	100	6	12.0 ± 0.2	10.3 ± 0.6	3.10 ± 0.28	4.58 ± 0.08	2.132	4.65	3.28
	3000	100	48	7.76 ± 0.28	8.75 ± 0.29	2.78 ± 0.04	4.00 ± 0.08	2.135	4.71	3.28
	3000	100	120	6.32 ± 0.39	8.52 ± 0.74	2.45 ± 0.13	3.42 ± 0.17	2.138	4.76	3.34
	4000	50	1	43.0 ± 1.4	25.8 ± 0.6	12.2 ± 0.4	17.1 ± 0.6	2.140	4.45	4.19
	4000	50	6	30.5 ± 2.9	24.8 ± 2.3	10.6 ± 1.2	15.7 ± 0.3	2.153	4.51	4.12
	4000	50	48	19.7 ± 0.6	21.5 ± 2.6	9.75 ± 0.75	13.7 ± 1.3	2.148	4.52	4.11
	4000	50	120	15.9 ± 0.9	20.1 ± 0.7	9.85 ± 0.92	13.7 ± 0.2	2.140	4.45	4.15
MgSiO ₃	2200	550	1	3.53 ± 1.03	2.59 ± 0.27	0.36 ± 0.01	0.47 ± 0.01	2.110	4.74	2.47
	2200	550	6	2.55 ± 0.24	2.04 ± 0.05	0.25 ± 0.03	0.33 ± 0.01	2.111	4.82	2.44
	2200	550	48	1.54 ± 0.25	1.81 ± 0.06	0.24 ± 0.01	0.33 ± 0.01	2.111	4.79	2.50
	2200	550	120	1.15 ± 0.11	1.52 ± 0.13	0.17 ± 0.01	0.25 ± 0.01	2.115	4.85	2.49
	2500	450	1	5.30 ± 0.35	3.97 ± 0.25	0.60 ± 0.01	0.81 ± 0.05	2.123	4.81	2.88
	2500	450	6	4.69 ± 0.10	4.08 ± 0.05	0.70 ± 0.05	0.99 ± 0.01	2.120	4.74	2.82
	2500	450	48	3.39 ± 0.33	3.82 ± 0.48	0.57 ± 0.04	0.76 ± 0.03	2.121	4.78	2.82
	2500	450	120	2.60 ± 0.22	3.36 ± 0.24	0.56 ± 0.02	0.73 ± 0.01	2.115	4.70	2.83
	3000	300	1	14.3 ± 0.8	9.45 ± 1.07	2.50 ± 0.13	3.21 ± 0.03	2.128	4.64	3.33
	3000	300	6	10.5 ± 2.5	8.97 ± 0.34	2.01 ± 0.10	2.84 ± 0.10	2.128	4.64	3.36
	3000	300	48	6.72 ± 0.62	7.54 ± 0.51	1.74 ± 0.12	2.27 ± 0.10	2.128	4.65	3.28
	3000	300	120	5.49 ± 0.09	7.74 ± 0.39	1.73 ± 0.12	2.22 ± 0.10	2.125	4.65	3.34
	4000	150	1	41.1 ± 2.6	25.0 ± 2.9	10.5 ± 0.3	13.9 ± 0.5	2.143	4.47	4.28
	4000	150	6	28.6 ± 1.9	23.4 ± 2.2	9.90 ± 0.81	12.8 ± 0.2	2.136	4.40	4.30
	4000	150	48	18.7 ± 3.7	22.0 ± 1.9	9.63 ± 0.55	12.3 ± 1.0	2.142	4.46	4.25
	4000	150	120	15.8 ± 0.5	20.1 ± 1.1	8.63 ± 0.30	10.9 ± 0.4	2.143	4.47	4.27

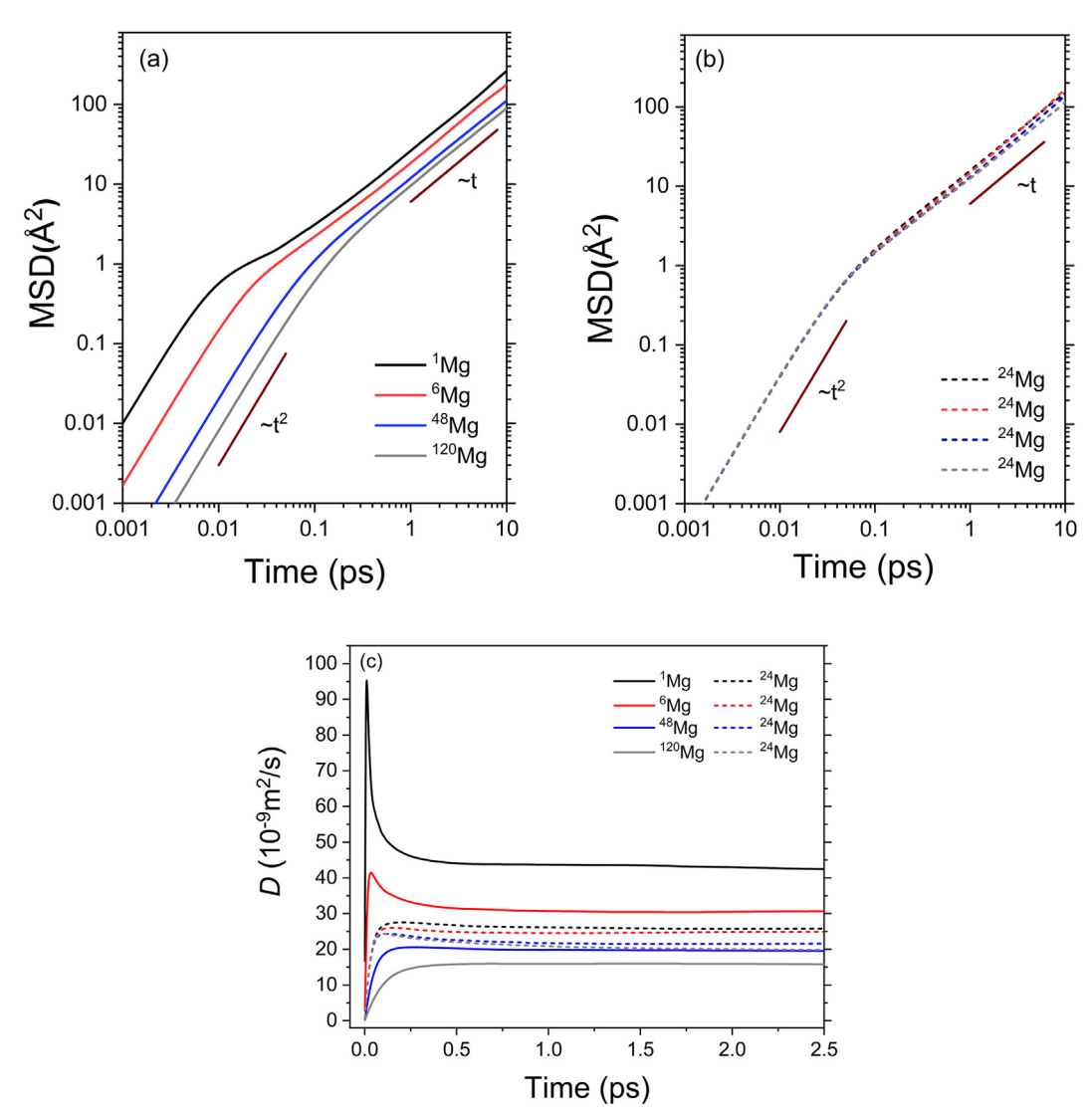


Fig. 1. (a and b) Mean square displacement (MSD) of several Mg isotopes (1 Mg, 6 Mg, 24 Mg, 48 Mg, 120 Mg) as a function of time in 1 Mg 24 MgSiO₄, 6 Mg 24 MgSiO₄, 48 Mg 24 MgSiO₄, and 120 Mg 24 MgSiO₄ melts (namely, half of 24 Mg atoms are substituted) at 4000 K and zero pressure (± 1 GPa). MSD curves of 24 Mg are expressed by dashed lines of the same color as their corresponding pseudo-isotopes in simulations. The ballistic regime (MSD $\sim t^2$) and diffusive regime (MSD $\sim t$) are also shown. (c) Diffusion coefficients of Mg isotopes (1 Mg, 6 Mg, 24 Mg, 48 Mg, 120 Mg) calculated from the corresponding MSD curves in (a and b).

in MgSiO₃ melts, which becomes more evident at lower temperatures.

3.2. Dependence of β on the substitution ratio, finite size, and exchange-correlation functional

The plots of $ln(D_{24}/D_{\alpha})$ versus $ln(M_{\alpha}/M_{24})$ in Mg₂SiO₄ melts with different ratios of Mg atoms substituted at 4000 K around zero pressure are shown in Fig. 2a. Calculated β values from linear regression lines are 0.158 \pm 0.019 for '6sub' (6 out of 32 ²⁴Mg atoms substituted), 0.154 \pm 0.004 for '16sub' (half substitution), 0.157 \pm 0.020 for '24sub' (24 out of 32 ²⁴Mg atoms substituted), and 0.272 \pm 0.004 for '32sub' (full substitution). No significant difference is found between partial substitution

groups. However, the β for Mg isotopes of full substitution (32sub) is much larger than the three β values under partial substitutions. The overestimation of β under full substitution is also seen in MgSiO₃ melts. As shown in Fig. 2b, calculated β values are 0.158 ± 0.009 for '8sub_80' (half substitution) and 0.253 ± 0.005 for '16sub_80' (full substitution). The two β values under full substitution are comparable to the results of Liu et al. (2018) in which doubled-size supercells were used, suggesting that finite size effect on β may be negligible when compared with 80 and 112 atom simulation cells. The β calculated in the doubled-size supercell (32MgSiO₃ units, total 160 atoms) with half (16/32) of ²⁴Mg atoms substituted is 0.151 \pm 0.008 (Fig. 2b), indicating that the finite size effect on β is insignificant within uncertainty as well. The β derived using GGA-PBE

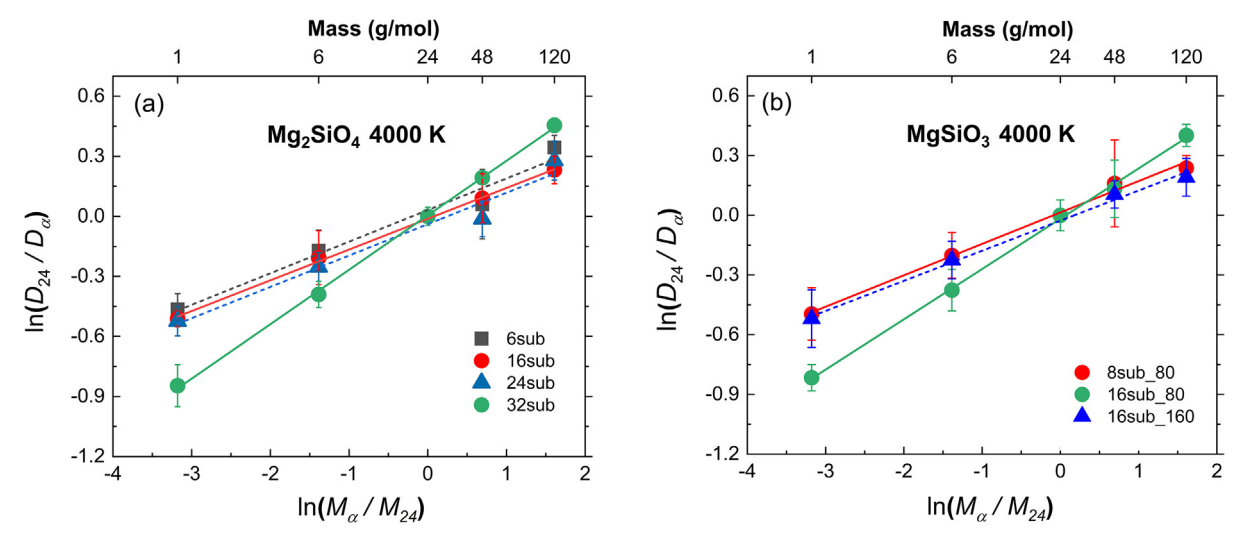


Fig. 2. (a) $ln(D_{24}/D_z)$ as a function of $ln(M_x/M_{24})$ in Mg₂SiO₄ melts with different fractions of 24 Mg atoms substituted by pseudo-isotopes (1 Mg, 6 Mg, 48 Mg, 120 Mg) at 4000 K and 0 GPa (± 1 GPa). '6sub' represents that 6 out of 32 24 Mg atoms were substituted. '32sub' represents that all 24 Mg atoms were substituted. M_x represents the pseudo-mass of Mg isotopes (1, 6, 24, 48 and 120 g/mol), and D_x is the corresponding diffusion coefficient. The β values calculated from linear fitting are 0.158 ± 0.019 for '6sub', 0.154 ± 0.004 for '16sub', 0.157 ± 0.020 for '24sub', and 0.272 ± 0.004 for '32sub'. (b) $ln(D_{24}/D_x)$ as a function of $ln(M_x/M_{24})$ in MgSiO₃ melts at 4000 K and 0 GPa (± 1 GPa). '8sub_80' represents that 8 out of 16 24 Mg atoms were substituted. '16sub_80' represents that all 24 Mg atoms were substituted. '16sub_160' represents the results of simulations doubled in system size (32MgSiO₃ units, total 160 atoms) with half (16/32) of 24 Mg atoms substituted. The calculated β values are 0.158 ± 0.009 for '8sub_80', 0.253 ± 0.005 for '16sub_80', and 0.151 ± 0.008 for '16sub_160'.

functional are 0.177 ± 0.008 and 0.173 ± 0.010 for Mg₂SiO₄ and MgSiO₃ melts at 4000 K (Fig. S3), respectively, suggesting the choice of exchange-correlation functional has a small systematic effect on the value of β .

3.3. Temperature dependence of Mg pseudo-isotope diffusivities

The calculated diffusion coefficients of Mg pseudo-isotopes in Mg₂SiO₄ and MgSiO₃ melts around zero pressure at 2200, 2500, 3000, and 4000 K are given in Table 1. The diffusivities of Mg pseudo-isotopes display a positive correlation with temperature and a negative correlation with mass (Fig. 3a & c). Meanwhile, the diffusivities of ²⁴Mg display a negative correlation with the mass of the other Mg pseudo-isotope (Fig. 3b & d). The linear trends in the logarithmic plot can be described by the Arrhenius relation:

$$D_{\alpha} = D_{0\alpha} exp \left[\frac{-E_{\alpha}}{RT} \right] \tag{6}$$

where R is the gas constant, α represents Mg isotope, and the fit parameters are given in Table 2. For 1 Mg, 6 Mg, 48 Mg, and 120 Mg, the predicted pre-exponential factor $(D_{0\alpha})$ decreases with increasing Mg isotopic mass. The predicted activation energies (E_{α}) do not show any definite trend with mass and remain around 88 and 100 kJ/mol for Mg₂SiO₄ and MgSiO₃ melts, respectively. These results are comparable to previous first-principles computations (Karki, 2010; Ghosh and Karki, 2011).

3.4. Pressure dependence of Mg pseudo-isotope diffusivities

The calculated pressure profiles of diffusional Mg isotope fractionation in Mg_2SiO_4 melts depict compression-induced suppression of diffusivities (Table 3). The lighter Mg-isotopes display relatively higher diffusion rates than those of the heavier ones at all pressures. Meanwhile, the diffusivities of ^{24}Mg display a negative correlation with the mass of the other Mg pseudo-isotopes.

3.5. Temperature, pressure, and composition dependence of β

In addition to the calculated set of β values based on Eq. (1) for Mg isotopes in Mg₂SiO₄ and MgSiO₃ melts at each temperature using the direct FPMD diffusivity results, we can also extract the diffusion coefficients of Mg isotopes according to the fitted Arrhenius relation (Table 2) and then derive another set of β values. We report the fitted results in the plots of β vs. *IIT* (Fig. 4a). The calculated β values from the direct FPMD data and from Arrhenius relation display a same linear correlation with *IIT* for MgSiO₃ and Mg₂SiO₄ melts, respectively, i.e.

$$Mg_2SiO_4: \beta$$

= $(0.210 \pm 0.013) - (0.024 \pm 0.004)$
 $\times 10^4/T(2200 \text{ K}$
 $< T < 4000 \text{ K}, 0 \text{ GPa}).$ (7)

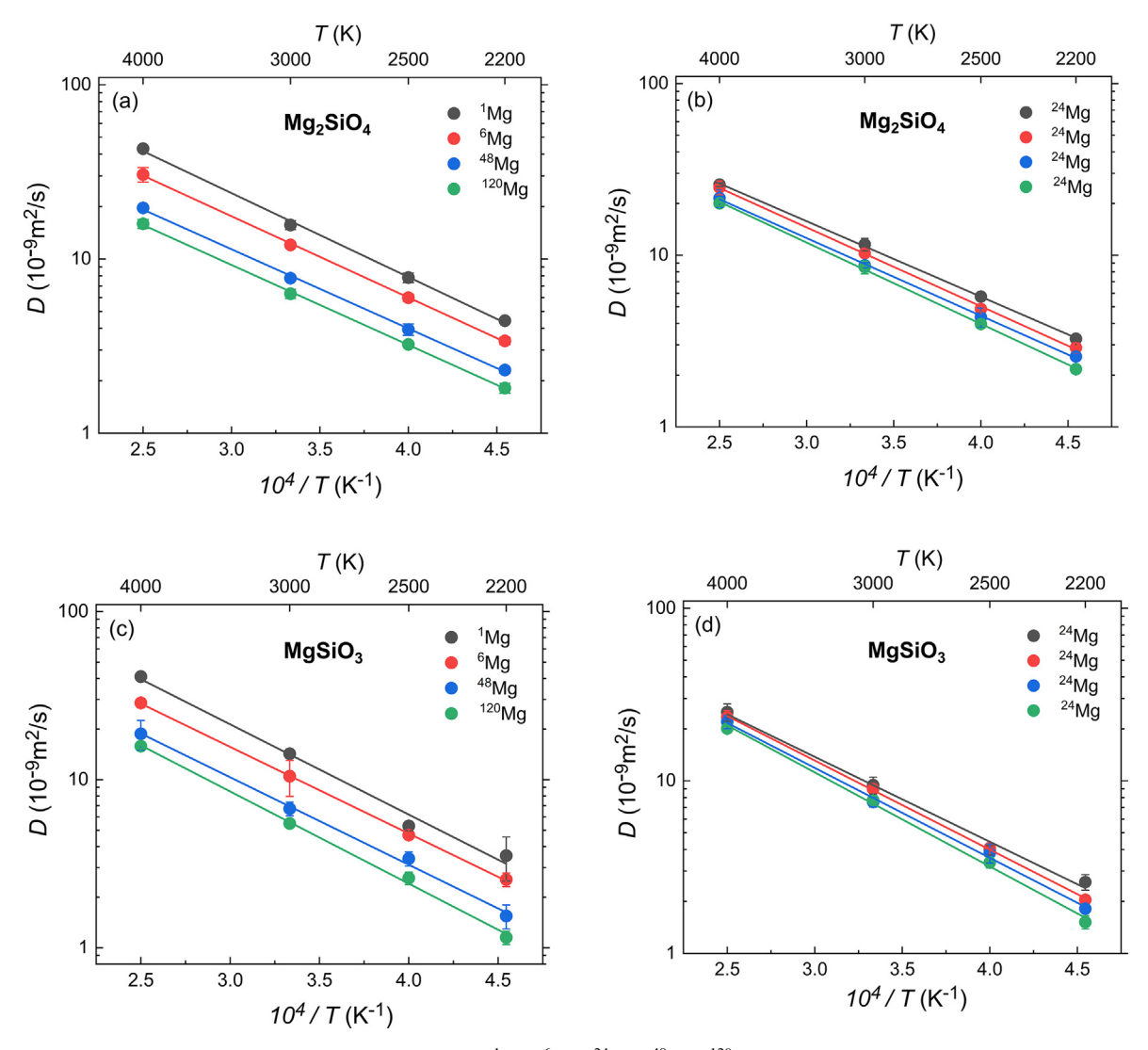


Fig. 3. (a–d) Diffusion coefficients of several Mg isotopes (1 Mg, 6 Mg, 24 Mg, 48 Mg, 120 Mg) as a function of temperature in Mg₂SiO₄ and MgSiO₃ melts with half of 24 Mg substituted around zero pressure (± 1 GPa). Diffusion coefficients of 24 Mg are expressed by the same solid circles as their corresponding pseudo-isotopes in simulations.

Table 2 Arrhenius fit parameters for the temperature variations of the diffusivities of different Mg isotopes (with mass M_{α}) in Mg₂SiO₄ and MgSiO₃ melts around zero pressure (± 1 GPa) under half substitution of ²⁴Mg.

			-			
	M_{α} (g/mol)	$D_{0\alpha} (10^{-9} \text{m}^2/\text{s})$	E_{α} (kJ/mol)	M_{α} (g/mol)	$D_{0\alpha} (10^{-9} \text{ m}^2/\text{s})$	E_{α} (kJ/mol)
Mg ₂ SiO ₄	1	664 ± 77	92.2 ± 2.6	24	329 ± 19	84.2 ± 1.3
	6	440 ± 21	89.2 ± 1.1	24	349 ± 25	88.1 ± 1.6
	48	263 ± 21	87.1 ± 1.8	24	287 ± 18	86.6 ± 1.4
	120	220 ± 12	87.8 ± 1.3	24	313 ± 22	90.7 ± 1.6
MgSiO ₃	1	872 ± 290	102.8 ± 7.5	24	413 ± 99	94.3 ± 5.4
	6	551 ± 27	98.7 ± 1.1	24	463 ± 29	98.8 ± 1.4
	48	376 ± 65	99.6 ± 3.9	24	435 ± 67	99.8 ± 3.5
	120	376 ± 59	105.0 ± 3.6	24	483 ± 84	104.3 ± 3.9

Diffusivities of Mg isotopes (with mass Mz), Si and O, Mg—O bond length, coordination number, and bond break rate in Mg₂SiO₄ melts at 3000 K under 8.1 and 17 GPa with half of ²⁴Mg substituted. Noted that the results at 0 GPa are given in Table

	P (GPa)	Time (ps)	M_{α} (g/mol)	$D_{\alpha} (10^{-9} \text{ m}^2/\text{s})$	$D_{Mg}^{24} (10^{-9} \text{ m}^2/\text{s})$	$D_{Si} (10^{-9} \text{ m}^2/\text{s})$	$D_O (10^{-9} \text{ m}^2/\text{s})$	$d_{Mg extit{-}O}\left(\mathring{\mathrm{A}} ight)$	Z_{Mg-O}	$1/ au_{Mg-O} \ (\mathrm{ps}^{-1})$
${ m Mg}_2{ m SiO}_4$	8.1	150	1	8.57 ± 0.82	6.46 ± 0.32	2.52 ± 0.19	4.27 ± 0.12	2.139	5.65	3.44
	8.1	150	9	6.51 ± 0.40	6.13 ± 0.61	2.17 ± 0.09	3.65 ± 0.07	2.139	5.72	3.49
	8.1	150	48	4.91 ± 0.13	5.68 ± 0.21	1.93 ± 0.05	3.30 ± 0.09	2.138	5.65	3.47
	8.1	150	120	4.11 ± 0.17	4.94 ± 0.63	1.77 ± 0.07	2.97 ± 0.08	2.139	5.73	3.46
	17.0	150		5.60 ± 0.59	4.37 ± 0.11	2.02 ± 0.09	3.32 ± 0.09	2.129	6.17	3.40
	17.0	150	9	4.36 ± 0.44	4.03 ± 0.29	1.72 ± 0.08	2.98 ± 0.05	2.130	6.27	3.44
	17.0	150	48	2.98 ± 0.16	3.07 ± 0.27	1.47 ± 0.06	2.70 ± 0.05	2.123	6.19	3.42
	17.0	150	120	2.59 ± 0.34	2.68 ± 0.06	1.23 ± 0.05	2.45 ± 0.01	2.122	60.9	3.42

$$MgSiO_3: \beta$$

= $(0.203 \pm 0.034) - (0.018 \pm 0.009)$
 $\times 10^4 / T(2200K)$
 $< T < 4000 \text{ K. 0 GPa}$, (8)

The errors of intercept and slope are given by the linear fitting of direct FPMD data.

The β values in Mg₂SiO₄ melts at 3000 K under upper mantle pressures are calculated using the direct FPMD diffusivity results. As shown in Fig. 4b, the calculated β show a near linear negative correlation with pressure, i.e.

$$Mg_2SiO_4: \beta$$

= (0.131 ± 0.002)
- $(0.004 \pm 0.000)P(0 \text{ GPa}$
 $< P < 17 \text{ GPa}, 3000 \text{ K}).$ (9)

4. DISCUSSION

4.1. Comparison with previous studies

Based on FPMD simulations, Liu et al. (2018) calculated β for Mg isotopes in Mg2SiO₄ and MgSiO₃ melts around zero pressure. Their 4000 K results for Mg₂SiO₄ and MgSiO₃ melts are, respectively, 0.257 ± 0.012 and 0.272 ± 0.005 , which are consistent with our FPMD values of 0.272 ± 0.004 in Mg₂SiO₄ melt and 0.253 ± 0.005 in MgSiO₃ melt (Fig. 2) around zero pressure under full substitution. However, these β values under full substitution are much larger than the results of partial substitution under which the interaction between Mg isotopes was considered. The reason why a full substitution approach leads to the overestimation of β can be qualitatively explained by a simplified example as shown in Fig. 5. Compared to the two separate systems with pure ²⁴Mg and pure ²⁶Mg, respectively (Fig. 5a), mixing of the two Mg isotopes results in the decrease of diffusivity in ²⁴Mg and the increase of diffusivity in ²⁶Mg, shrinking the difference between their diffusivities (Fig. 5b & c). It is because the mobility of one Mg ion is influenced by other ambient Mg ions even though they do not bond with each other directly. Furthermore, we found out that the fractions of substitution do not significantly change the β because a larger fraction of $^{26}{\rm Mg}$ results in the decrease of diffusivities in both 24Mg and ²⁶Mg (Fig. 5c). In terms of diffusion experiments of isotopes, the difference between full substitution and partial substitution shown here implies that β for major elements will be over-estimated if it is derived from two separate diffusion experiments with pure light isotopes and pure heavy isotopes, respectively, although no one has yet done such experiments to calibrate β for major elements.

Previous experiments reported a β of 0.050 ± 0.005 in basalt-rhyolite melts at 1400 °C (Richter et al., 2008) and a β of 0.100 ± 0.010 in albite-diopside melts at 1450 °C (Watkins et al., 2011). Assuming the temperature dependence of β predicted in the present study is also valid at lower temperatures, our calculated β in Mg₂SiO₄ and MgSiO₃ melts are 0.067 and 0.095, respectively, at 1400 °C, and 0.071 and 0.099, respectively, at 1450 °C.

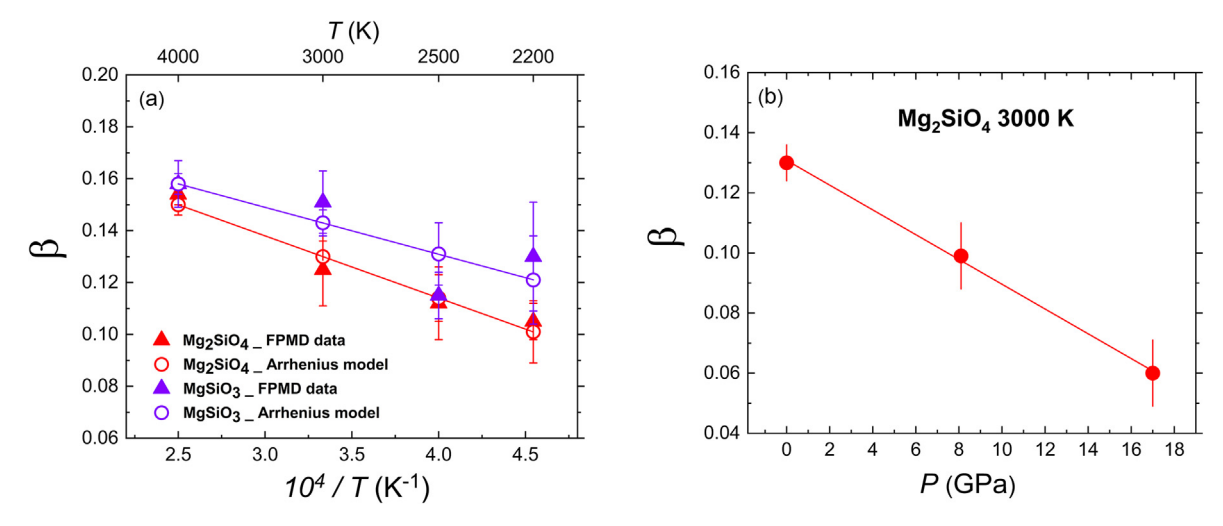


Fig. 4. (a) Correlation of β with the inverse of temperature (*IIT*) calculated based on original (direct FPMD) diffusivity data and recalculated diffusivity data by Arrhenius model. Noted that original diffusivity data and recalculated diffusivity data give the same linear fitting results. (b) Correlation of β with pressure with the red line being a linear fit.

These results are in broad agreement with experimental data. The most likely explanation of the remaining discrepancies in β values is chemical composition effect (Watkins et al., 2011). Our FPMD results also show that the β decreases nearly linearly with pressure increasing from 0 to 17 GPa in Mg₂SiO₄ melt at 3000 K. The negative correlation between β and pressure was also predicted by a classical MD simulation study (Goel et al., 2012). Their results for Mg isotopes in MgSiO₃ melts at 4000 K are $0.135 \pm 0.008, 0.092 \pm 0.006$, and 0.084 ± 0.016 at 0, 25, and 50 GPa, respectively. Their β value at 4000 K and 0 GPa is only slightly smaller than our calculated β of 0.158 ± 0.009 in MgSiO₃ melt (Fig. 2), but the β -P behavior shows a somewhat different trend compared to our results. In addition to the composition effect between Mg₂SiO₄ and MgSiO₃ melts, a possible explanation is that, unlike classical MD simulations that use empirical potentials, our FPMD method handles interactive forces quantum mechanically.

4.2. Correlation between β and solvent-normalized diffusivity

As water molecules play the role of solvent in aqueous solutions, the $(Si, Al)O_4^{4-}$ tetrahedral units are usually regarded as the solvent ion in silicate melts. Previous experiments and classical MD simulations of silicate melts and aqueous solutions showed that the magnitude of diffusive separation of isotopes (β) has a broadly positive correlation solvent-normalized diffusivity $(D_{\text{solute}}/D_{\text{solvent}})$ (Watkins et al., 2011, 2017). This implies that, the easier the cation can decouple from the motion of liquid matrix, the larger isotope fractionation by diffusion can be. At same temperatures, we observed a similar positive correlation between β for Mg isotopes and $D_{\text{Mg}}/D_{\text{Si}}$ (Fig. 6a). However, with temperature decreasing, β decreases with increasing $D_{\text{Mg}}/D_{\text{Si}}$ in Mg2SiO₄ and MgSiO₃ melts, respectively (Fig. 6a). To clarify, we used β values calculated from recalculated diffusivity data by Arrhenius model in all figures in the DISCUSSION part. The observed opposite relationship between β and $D_{\rm Mg}/D_{\rm Si}$ can be explained if $D_{\rm Mg}/D_{\rm Si}$ cannot fully represent the extent of coupling between diffusing Mg and the motion of melt matrix. Although $D_{\rm Mg}/D_{\rm Si}$ is higher at lower temperatures, $D_{\rm Mg}$ itself is smaller, which means that it takes Mg atoms longer time to hop from site to site. The previously observed positive correlation between β and $D_{\rm i}/D_{\rm Si}$ (Fig. 6b) is probably due to similar temperatures (~1350–1500 °C) used in experiments except for element Li in Holycross et al. (2018). In conclusion, this positive correlation is applicable only at a constant or narrowly defined temperature range.

4.3. Atomic mechanism of β

Although D_i/D_{Si} is not a good indicator of β over a wide temperature range, the basic idea that the extent of coupling between diffusing ions and melt matrix determines the β may still hold. Here we examine the effects of structural and dynamical properties on β . The influence of melt structure on diffusive separation of Mg isotopes can be assessed by examining the correlations of β with Mg–O bond length, Mg-O coordination number, and force constant of Mg. Force constants of Mg were calculated by extracting 20 snapshots of respective FPMD simulations at least 2 ps apart and using finite displacement scheme by fixing all atoms except the Mg of interest whose position was optimized. Force constants of Mg for the 16 sites in MgSiO₃ snapshots and 32 sites in Mg₂SiO₄ snapshots were averaged, respectively. Mg-O bond break rates (the inverse of bond lifetime) were computed to investigate the effect of dynamical properties on β .

As shown in Fig. 7, if we only consider temperature variations of β in Mg₂SiO₄ and MgSiO₃ melts, respectively, β positively correlates with Mg—O bond length (Fig. 7a), and negatively correlates with Mg—O coordination number (Fig. 7b), and negatively correlates with force constant of Mg (Fig. 7c), and positively correlates with Mg—O bond

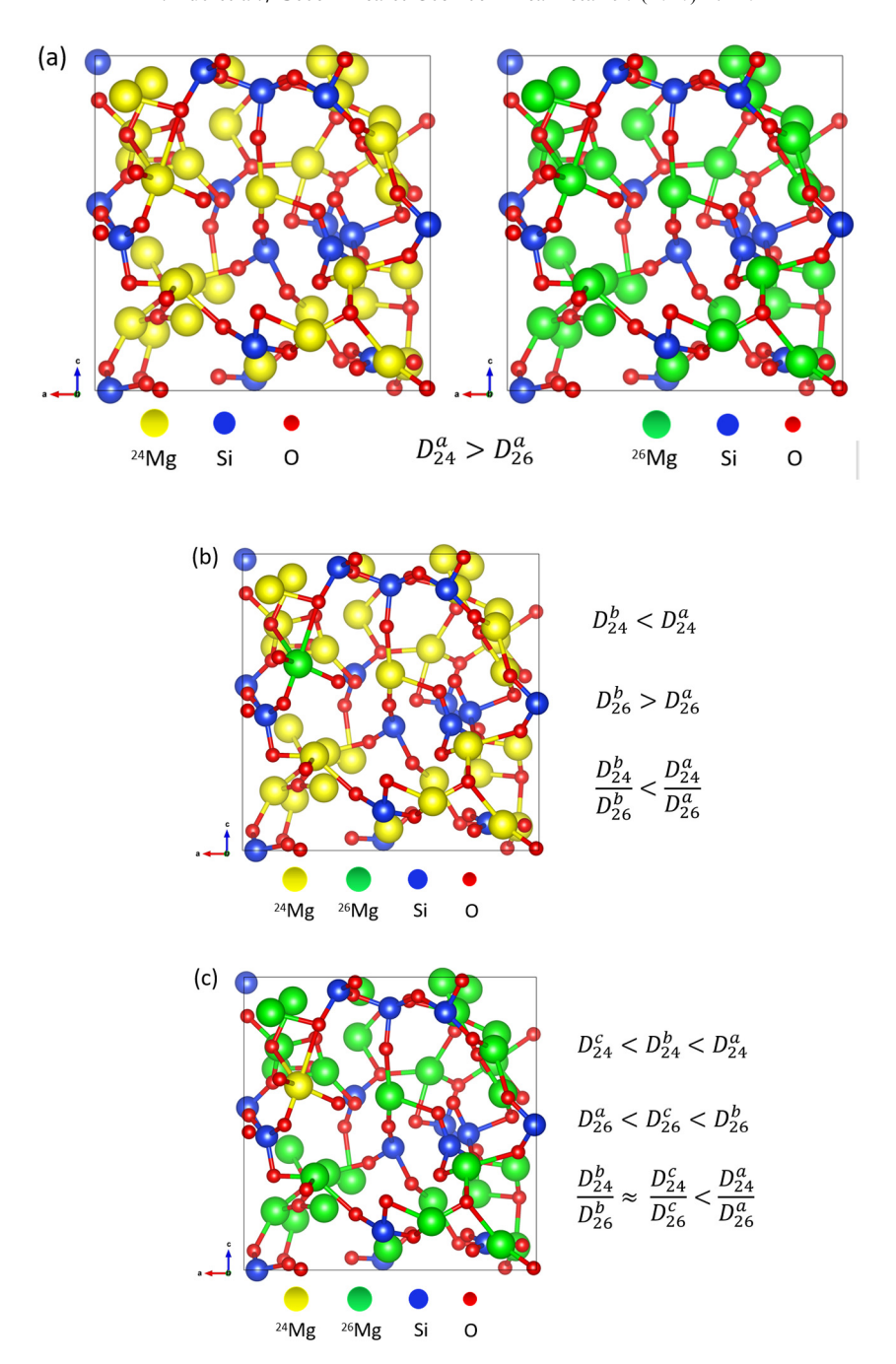


Fig. 5. A simplified example showing the qualitative changes of diffusivities of Mg isotopes at different substitution fractions. (a) full substitution; (b) substituting one ²⁴Mg with ²⁶Mg. (c) Only one ²⁴Mg is not substituted.

break rate (Fig. 7d). All the four correlations imply that the stronger Mg couples with melt matrix, the smaller diffusional Mg isotope fractionation will be. However, it is questionable whether some of the four correlations are pseudo or indirect. In considering pressure variations of β in Mg₂-SiO₄ melts, we can clearly see that Mg—O bond length and bond break rate fail to show the positive correlations with β . In Fig. 7a, Mg—O bond length in Mg₂SiO₄ melts at 3000 K increases from 2.134 \pm 0.003 Å at 0 GPa to 2.138 \pm 0.001 Å at 8.1 GPa, but the corresponding β decreases from 0.130 \pm 0.006 to 0.099 \pm 0.011. A similar

anomalous trend is also seen in the plot of β vs. Mg—O bond break rate (Fig. 7d), revealing that the negative correlation of β with residence times of water molecules found in aqueous solutions (Bourg and Sposito, 2007; Bourg and Sposito, 2008; Bourg et al., 2010) is not applicable to the case of melts at elevated pressures. Instead, the correlation of β with force constant of Mg remains broadly consistent. It is worth noting that although the characteristics such as, bond length, coordination number, and bond breaking rate are statistically very reliable, they depend on the choice of the cutoff distance used in calculating them. On the con-

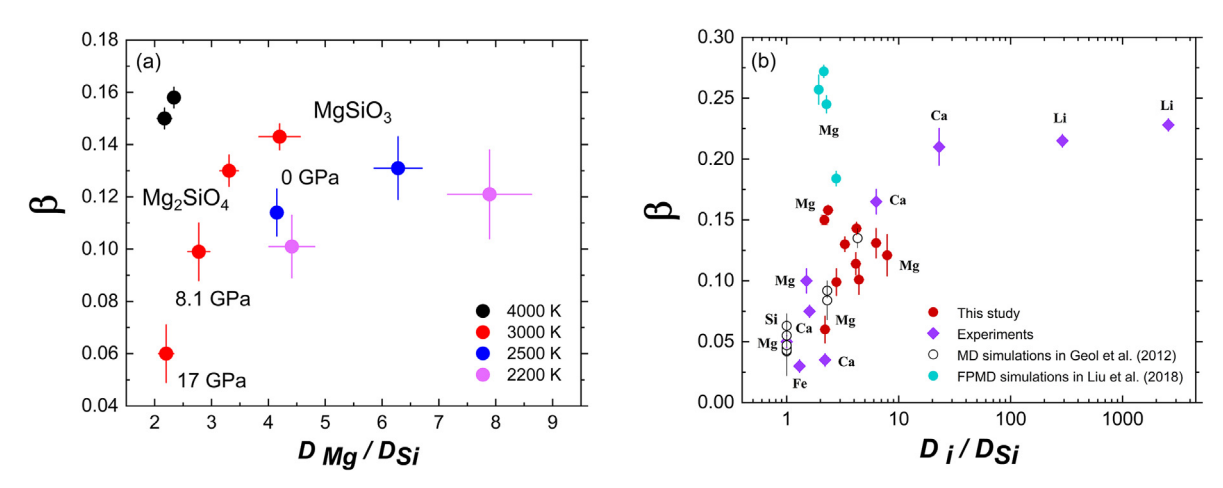


Fig. 6. Relationship of β with (a) $D_{\rm Mg}/D_{\rm Si}$ in Mg₂SiO₄ and MgSiO₃ melts at 4000, 3000, 2500, and 2000 K around zero pressure (± 1 GPa), as well as Mg₂SiO₄ melts at 3000 K under 8.1 and 17 GPa, and (b) $D_{\rm i}/D_{\rm Si}$ in silicate melts. Experimental data are from Richter et al. (2003, 2008, 2009b), Watkins et al. (2011), and Holycross et al. (2018).

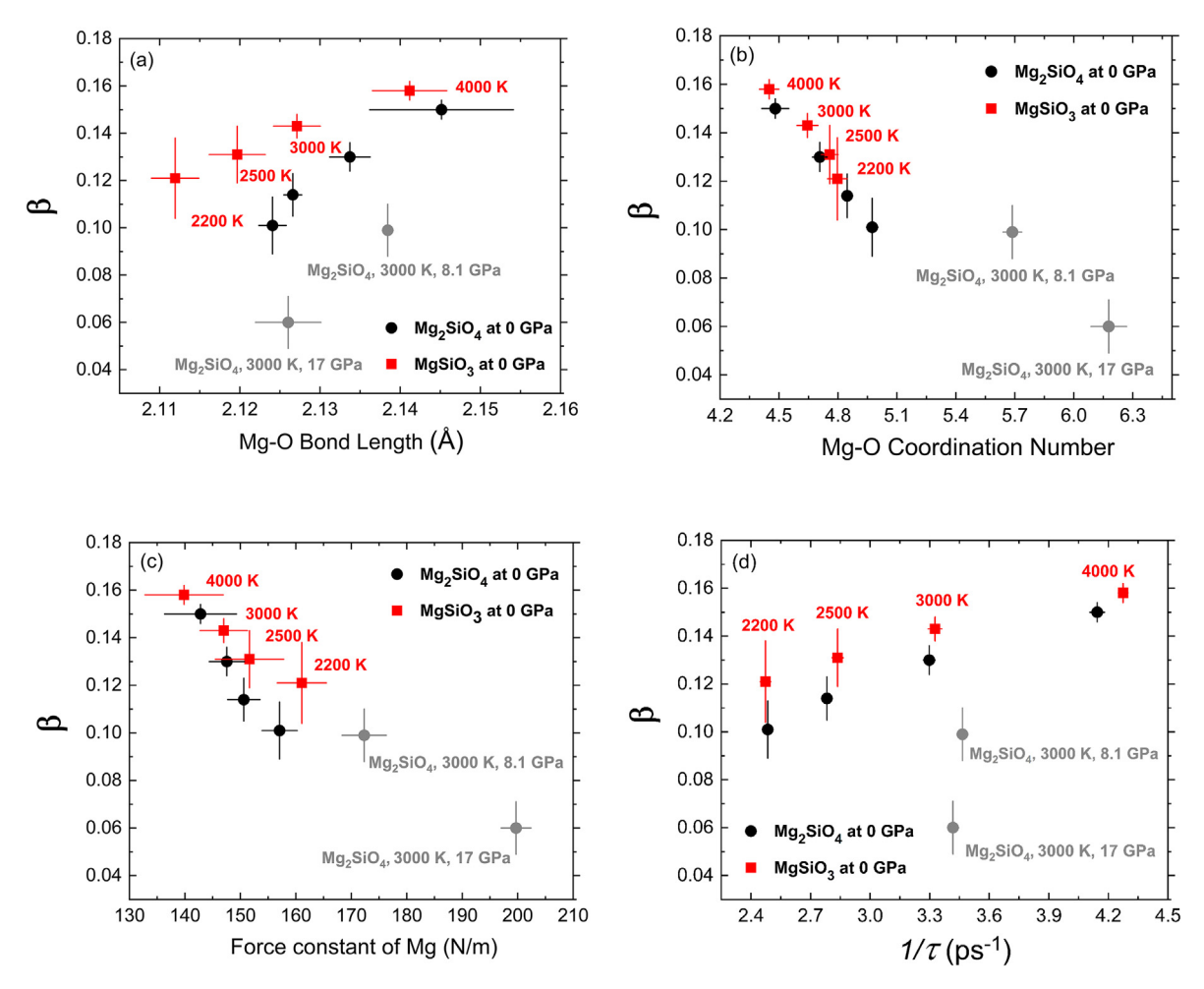


Fig. 7. Correlations of β with (a) Mg—O bond length, and (b) Mg—O coordination number, and (c) force constant of Mg, and (d) the inverse of average Mg—O bond lifetimes in Mg₂SiO₄ and MgSiO₃ melts at 4000, 3000, 2500, and 2000 K around zero pressure, as well as Mg₂SiO₄ melts at 3000 K under 8.1 and 17 GPa.

trary, calculation of force constant in quantum mechanical simulations involves optimization at the electronic level and is thus robust. We therefore stress that the force constant could be the intrinsic factor determining diffusional isotope fractionation, especially in considering temperature and pressure variations of β at the same time. More extensive FPMD simulations and explorations of theoretical basis of β may help to confirm the correlation.

4.4. Geological implications

Three common geochemical processes associated with isotope fractionation by chemical diffusion in silicate melts are crystal growth, bubble growth, and magma mixing. Using our computational results, we can estimate Mg isotope composition of a rapidly growing crystal from magma based on a diffusion-controlled crystal growth model (Watson and Müller, 2009). Bubble growth is not considered because Mg is not a volatile element. Discussion on isotope fractionation by chemical diffusion during magma mixing can be found in several previous studies (Chopra et al., 2012; Goel et al., 2012; Richter et al., 1999; Richter et al., 2003). Watson and Müller. (2009) proposed that non-equilibrium isotope fractionation could be significant during rapid crystal growth, which was confirmed by the observation of large kinetic Ca isotope fractionation (>2‰) in experimental and natural samples of plagioclase phenocrysts during magmatic plagioclase crystallization (Antonelli et al., 2019). Goel et al. (2012) briefly discussed Mg isotope fractionation during crystallization of olivine based on their calculated β in MgSiO₃ melt at 4000 K.

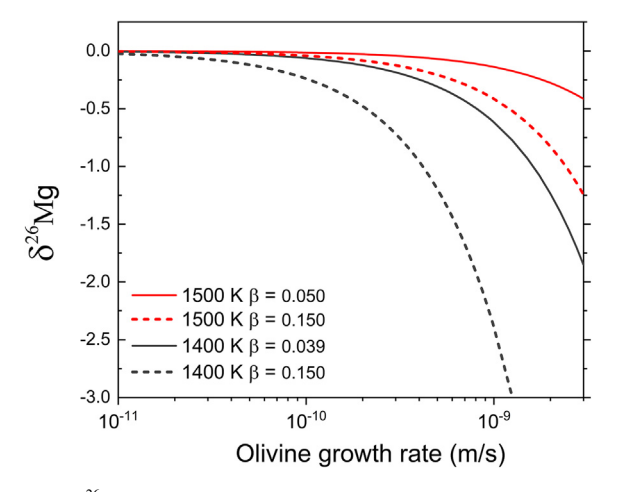


Fig. 8. $\delta^{26}Mg$ in an olivine phenocryst as a function of its growth rate. Diffusivities of normal Mg, $D_{Mg} = exp(-7.92 - 26222/T)$ (1543 K < T < 1753 K), are taken from experiments of olivine dissolution in basaltic melt (Zhang et al., 2010). The boundary layer thickness is assumed to be 100 µm. The olivine/melt partition coefficients for Mg are taken from logK = 3740/T - 1.87(1423 K < T < 1573 K)(Roeder Emslie, 1970). Necessary extrapolations of our calculated β and experimental data for D_{Mg} and K are used. The two solid lines are based on the extrapolated β using Eq. (7). The two dotted lines are based on the calculated β at 4000 K. The lines of same color represent same temperature.

Assuming equilibrium isotope fractionation is negligible and the boundary-layer thickness is small compared to crystal radius, an approximate solution of the steady-state $\delta^{26}Mg$ fractionation between olivine and crystal is (Watson and Müller, 2009):

$$\delta^{26} Mg = 1000 \left(1 - \frac{D_{26}}{D_{24}} \right) \left(\frac{R \times BL}{D_{26}} \right) (1 - K) \tag{10}$$

where D_{26} and D_{24} are the diffusivities of ²⁶Mg and ²⁴Mg in the melt, respectively, R is the olivine growth rate (m/s), BL is the boundary layer thickness (m), and K is the equilibrium partition coefficient of Mg in the olivine vs. the melt.

We calculated the $\delta^{26}Mg$ using extrapolated β based on Eq. (7) at 1500 and 1400 K. One of our goals was to check the effects of the temperature dependence of β on the $\delta^{26}Mg$. It is shown (Fig. 8) that the $\delta^{26}Mg$ of olivine becomes more negative with decreasing temperature at any given olivine growth rate mainly due to R/D value increases with decreasing temperatures. In contrast, ignoring the temperature dependence of β , i.e. using β calculated at 4000 K, would have resulted in a significant overestimation of the isotope fractionation between olivine and melt at 1500 and 1400 K. It is worth noting that Mg-Fe inter-diffusion during olivine growth also fractionates Mg isotopes, but in an opposite way. Newest single olivine crystal diffusion couple experiments estimated $\beta_{Mg} = 0.09 \pm 0.05$ without a resolvable temperature dependence at 1200, 1300, and 1400 °C (Sio et al., 2018). Possible similarities or differences between diffusive separation of isotopes in melts (or glasses) and in high-temperature crystals remain to be determined. In addition, we noticed that the calculated β in Mg₂SiO₄ melts decreases at a rate of about 0.004 per GPa at 3000 K, resulting from the stronger coupling between the mobility of Mg and the silicate melt network (Fig. 6a) and from the increasing force constants of Mg as pressure increases (Fig. 7c). Although the temperature (3000 K) we considered here do not readily apply for the natural silicate melts that may exist at shallower depths of the present-day Earth, a basic idea we can obtain is that the pressure dependence of β is insignificant in the Earth's crust but may become a concern once the pressure difference reaches several GPa.

5. CONCLUSIONS

We presented a partial substitution, pseudo-mass approach in calculating β for major elements in silicate melts based on FPMD simulations. The discrepancy between calculated β for Mg in previous FPMD simulations and in classical MD simulations or from experimental results is resolved after considering the interaction between Mg isotopes in melts. As long as the interaction between isotopes of the major element is considered by simultaneously putting pseudo-mass and normal-mass atoms in each simulation box, the specific substitution ratios yield no significant change. Our calculated β values for Mg in Mg2SiO₄ and MgSiO₃ melts around zero pressure decrease with decreasing temperature. The β in Mg2SiO₄ melts at 3000 K decreases with increasing pressure. A negative cor-

relation between the calculated β and solvent-normalized diffusivity ($D_{\rm Mg}/D_{\rm Si}$) from 4000 to 2200 K suggest that the previously proposed empirical positive correlation between β and solvent-normalized diffusivity only applies to data at a constant temperature. Among the four structural and dynamical properties of Mg, i.e., Mg—O bond length, Mg—O coordination number, force constant of Mg, and Mg—O bond break rate, force constant of Mg is found to be most consistent with the variations of β .

Declaration of Competing Interest

The authors declare that they have no known competing financial interests or personal relationships that could have appeared to influence the work reported in this paper.

ACKNOWLEDGMENTS

The research is supported by the Strategic Priority Research Program (B) of Chinese Academy of Sciences (XDB18010104) and National Science Foundation (EAR 1764140). High performance computing resources were provided by Louisiana State University. The authors are thankful to James Van Orman (A.E.) and two anonymous reviewers for their constructive comments and suggestions.

APPENDIX A. SUPPLEMENTARY MATERIAL

Supplementary data to this article can be found online at https://doi.org/10.1016/j.gca.2020.08.028.

REFERENCES

- Antonelli M. A., Mittal T., McCarthy A., Tripoli B., Watkins J. M. and DePaolo D. J. (2019) Ca isotopes record rapid crystal growth in volcanic and subvolcanic systems. *P. Natl. Acad. Sci. USA* 116, 20315–20321.
- Bajgain S., Ghosh D. B. and Karki B. B. (2015) Structure and density of basaltic melts at mantle conditions from firstprinciples simulations. *Nat. Commun.* 6.
- Bigeleisen J. and Mayer M. G. (1947) Calculation of equilibrium constants for isotopic exchange reactions. *J. Chem. Phys.* **15**, 261–267.
- Blochl P. E. (1994) Projector augmented-wave method. *Phys. Rev. B* **50**, 17953–17979.
- Bourg I. C., Richter F. M., Christensen J. N. and Sposito G. (2010) Isotopic mass dependence of metal cation diffusion coefficients in liquid water. *Geochim. Cosmochim. Acta* 74, 2249–2256.
- Bourg I. C. and Sposito G. (2007) Molecular dynamics simulations of kinetic isotope fractionation during the diffusion of ionic species in liquid water. *Geochim. Cosmochim. Acta* 71, 5583– 5589.
- Bourg I. C. and Sposito G. (2008) Isotopic fractionation of noble gases by diffusion in liquid water: molecular dynamics simulations and hydrologic applications. *Geochim. Cosmochim. Acta* 72, 2237–2247.
- Caracas R., Hirose K., Nomura R. and Ballmer M. D. (2019) Melt-crystal density crossover in a deep magma ocean. *Earth Planet. Sci. Lett.* **516**, 202–211.
- Ceperley D. M. and Alder B. J. (1980) Ground-state of the electron-gas by a stochastic method. *Phys. Rev. Lett.* **45**, 566–569.

- Chapman (1970). The mathematical theory of nonuniform gases: an account of the kinetic theory of viscosity, thermal, THE UNIV. PR.
- Chopra R., Richter F. M., Watson E. B. and Scullard C. R. (2012) Magnesium isotope fractionation by chemical diffusion in natural settings and in laboratory analogues. *Geochim. Cos-mochim. Acta* 88, 1–18.
- Clayton R. N., Hinton R. W. and Davis A. M. (1988) Isotopic variations in the rock-forming elements in meteorites. *Phil. Trans. Royal Spc. Lond.* A325, 483–501.
- Dauphas N., Teng F. Z. and Arndt N. T. (2010) Magnesium and iron isotopes in 2.7 Ga Alexo komatiites: mantle signatures, no evidence for Soret diffusion, and identification of diffusive transport in zoned olivine. *Geochim. Cosmochim. Acta* 74, 3274–3291
- Davis A. M., Hashimoto A., Clayton R. N. and Mayeda T. K. (1990) Isotope Mass Fractionation during Evaporation of Mg2sio4. *Nature* 347, 655–658.
- Dominguez G., Wilkins G. and Thiemens M. H. (2011) The Soret effect and isotopic fractionation in high-temperature silicate melts. *Nature* 473, 70–U134.
- Einstein A. (1956) Investigation on the Theory of the Brownian Movement. Courier Corporation.
- Fortin M. A., Watson E. B. and Stern R. (2017) The isotope mass effect on chlorine diffusion in dacite melt, with implications for fractionation during bubble growth. *Earth Planet. Sci. Lett.* **480.** 15–24.
- Fortin M. A., Watson E. B., Stern R. A. and Ono S. (2019) Experimental characterization of diffusive and Soret isotopic fractionation of sulfur in a reduced, anhydrous basaltic melt. *Chem. Geol.* **510**, 10–17.
- Ghosh D. B. and Karki B. B. (2011) Diffusion and viscosity of Mg2SiO4 liquid at high pressure from first-principles simulations. *Geochim. Cosmochim. Acta* 75, 4591–4600.
- Goel G., Zhang L. Q., Lacks D. J. and Van Orman J. A. (2012) Isotope fractionation by diffusion in silicate melts: Insights from molecular dynamics simulations. *Geochim. Cosmochim.* Acta 93, 205–213.
- Holycross M. E., Watson E. B., Richter F. M. and Villeneuve J. (2018) Diffusive fractionation of Li isotopes in wet, highly silicic melts. *Geochem. Perspect. Let.* 6, 39–42.
- Huang F., Chakraborty P., Lundstrom C. C., Holmden C., Glessner J. J. G., Kieffer S. W. and Lesher C. E. (2010) Isotope fractionation in silicate melts by thermal diffusion. *Nature* 464, 396–U389.
- Huang F., Lundstrom C. C., Glessner J., Ianno A., Boudreau A., Li J., Ferre E. C., Marshak S. and DeFrates J. (2009) Chemical and isotopic fractionation of wet andesite in a temperature gradient: experiments and models suggesting a new mechanism of magma differentiation. *Geochim. Cosmochim. Acta* 73, 729–749.
- Karki B. B. (2010) First-principles molecular dynamics simulations of silicate melts: structural and dynamical properties. *Theor. Comput. Methods Miner. Phys.: Geophys. Appl.* 71, 355–389.
- Knight K. B., Kita N. T., Mendybaev R. A., Richter F. M., Davis A. M. and Valley J. W. (2009) Silicon isotopic fractionation of CAI-like vacuum evaporation residues. *Geochim. Cosmochim. Acta* 73, 6390–6401.
- Kresse G. and Furthmüller J. (1996) Efficiency of ab-initio total energy calculations for metals and semiconductors using a plane-wave basis set. *Comput. Mater. Sci.* **6**, 15–50.
- Kresse G. and Joubert D. (1999) From ultrasoft pseudopotentials to the projector augmented-wave method. *Phys. Rev. B* **59**, 1758–1775.
- Lacks D. J., Goel G., Bopp C. J., Van Orman J. A., Lesher C. E. and Lundstrom C. C. (2012) Isotope fractionation by thermal diffusion in silicate melts. *Phys. Rev. Lett.* 108.

- Liu X. H., Qi Y. H., Zheng D. Y., Zhou C., He L. X. and Huang F. (2018) Diffusion coefficients of Mg isotopes in MgSiO3 and Mg2SiO4 melts calculated by first-principles molecular dynamics simulations. *Geochim. Cosmochim. Acta* 223, 364–376.
- McQuarrie D. A. (1976) *Statistical Mechanics*. Harper and Row, New York.
- Mendybaev R. A., Williams C. D., Spicuzza M. J., Richter F. M., Valley J. W., Fedkin A. V. and Wadhwa M. (2017) Thermal and chemical evolution in the early Solar System as recorded by FUN CAIs: Part II - Laboratory evaporation of potential CMS-1 precursor material. *Geochim. Cosmochim. Acta* 201, 49– 64.
- Oeser M., Dohmen R., Horn I., Schuth S. and Weyer S. (2015) Processes and time scales of magmatic evolution as revealed by Fe-Mg chemical and isotopic zoning in natural olivines. *Geochim. Cosmochim. Acta* **154**, 130–150.
- Richter F. M., Dauphas N. and Teng F. Z. (2009a) Non-traditional fractionation of non-traditional isotopes: evaporation, chemical diffusion and Soret diffusion. *Chem. Geol.* 258, 92–103.
- Richter F. M., Davis A. M., DePaolo D. J. and Watson E. B. (2003) Isotope fractionation by chemical diffusion between molten basalt and rhyolite. *Geochim. Cosmochim. Acta* 67, 3905–3923.
- Richter F. M., Davis A. M., Ebel D. S. and Hashimoto A. (2002) Elemental and isotopic fractionation of Type B calcium-, aluminum-rich inclusions: experiments, theoretical considerations, and constraints on their thermal evolution. *Geochim. Cosmochim. Acta* 66, 521–540.
- Richter F. M., Janney P. E., Mendybaev R. A., Davis A. M. and Wadhwa M. (2007) Elemental and isotopic fractionation of Type BCAI-like liquids by evaporation. *Geochim. Cosmochim.* Acta 71, 5544–5564.
- Richter F. M., Liang Y. and Davis A. M. (1999) Isotope fractionation by diffusion in molten oxides. *Geochim. Cosmochim. Acta* 63, 2853–2861.
- Richter F. M., Watson E. B., Chaussidon M., Mendybaev R., Christensen J. N. and Qiu L. (2014) Isotope fractionation of Li and K in silicate liquids by Soret diffusion. *Geochim. Cos-mochim. Acta* 138, 136–145.
- Richter F. M., Watson E. B., Mendybaev R., Dauphas N., Georg B., Watkins J. and Valley J. (2009b) Isotopic fractionation of the major elements of molten basalt by chemical and thermal diffusion. *Geochim. Cosmochim. Acta* 73, 4250–4263.
- Richter F. M., Watson E. B., Mendybaev R. A., Teng F. Z. and Janney P. E. (2008) Magnesium isotope fractionation in silicate melts by chemical and thermal diffusion. *Geochim. Cosmochim. Acta* 72, 206–220.
- Roeder P. L. and Emslie R. F. (1970) Olivine-liquid equilibrium. *Contrib. Miner. Petrol.* **19**, 275–289.
- Sio C. K., Roskosz M., Dauphas N., Bennett N. R., Mock T. and Shahar A. (2018) The isotope effect for Mg-Fe interdiffusion in olivine and its dependence on crystal orientation, composition and temperature. *Geochim. Cosmochim. Acta* 239, 463–480.
- Sio C. K. I., Dauphas N., Teng F. Z., Chaussidon M., Helz R. T. and Roskosz M. (2013) Discerning crystal growth from diffusion profiles in zoned olivine by in situ Mg-Fe isotopic analyses. *Geochim. Cosmochim. Acta* 123, 302–321.

- Solomatova N. V. and Caracas R. (2019) Pressure-induced coordination changes in a pyrolitic silicate melt from ab initio molecular dynamics simulations. *J. Geophys. Res.-Sol. Ea.* 124, 11232–11250.
- Stixrude L. and Karki B. (2005) Structure and freezing of MgSiO3 liquid in Earth's lower mantle. *Science* **310**, 297–299.
- Teng F. Z., Dauphas N., Helz R. T., Gao S. and Huang S. C. (2011) Diffusion-driven magnesium and iron isotope fractionation in Hawaiian olivine. *Earth Planet. Sci. Lett.* 308, 317–324.
- Teng F. Z., McDonough W. F., Rudnick R. L. and Walker R. J. (2006) Diffusion-driven extreme lithium isotopic fractionation in country rocks of the Tin Mountain pegmatite. *Earth Planet. Sci. Lett.* 243, 701–710.
- Urey H. C. (1947) The thermodynamic properties of isotopic substances. *J. Chem. Soc.*, 562–581.
- Van Orman, J.A., Krawczynski, M.J., 2015. Theoretical constraints on the isotope effect for diffusion in minerals. Geochim Cosmochim Ac 164, 365–381.
- Wang J. (1994) Chemical and isotopic fractionation during the evaporation of synthetic forsterite and material of solar composition. Ph. D. thesis. Univ. Chicago.
- Watkins J. M., DePaolo D. J., Huber C. and Ryerson F. J. (2009) Liquid composition-dependence of calcium isotope fractionation during diffusion in molten silicates. *Geochim. Cosmochim.* Acta 73, 7341–7359.
- Watkins J. M., DePaolo D. J., Ryerson F. J. and Peterson B. T. (2011) Influence of liquid structure on diffusive isotope separation in molten silicates and aqueous solutions. *Geochim. Cosmochim. Acta* 75, 3103–3118.
- Watkins J. M., DePaolo D. J. and Watson E. B. (2017) Kinetic fractionation of non-traditional stable isotopes by diffusion and crystal growth reactions. *Non-Tradit. Stable Isotopes* 82, 85– 125.
- Watkins J. M., Liang Y., Richter F., Ryerson F. J. and DePaolo D. J. (2014) Diffusion of multi-isotopic chemical species in molten silicates. *Geochim. Cosmochim. Acta* 139, 313–326.
- Watson, E.B., 2017. Diffusive fractionation of volatiles and their isotopes during bubble growth in magmas. Contrib Mineral Petr 172.
- Watson E. B. and Müller T. (2009) Non-equilibrium isotopic and elemental fractionation during diffusion-controlled crystal growth under static and dynamic conditions. *Chem. Geol.* **267.** 111–124.
- Wu H. J., He Y. S., Teng F. Z., Ke S., Hou Z. H. and Li S. G. (2018) Diffusion-driven magnesium and iron isotope fractionation at a gabbro-granite boundary. *Geochim. Cosmochim. Acta* 222, 671–684.
- Zhang J. J., Huang S. C., Davis A. M., Dauphas N., Hashimoto A. and Jacobsen S. B. (2014) Calcium and titanium isotopic fractionations during evaporation. *Geochim. Cosmochim. Acta* 140, 365–380.
- Zhang Y., Ni H. and Chen Y. (2010) Diffusion data in silicate melts. Rev. Mineral. Geichem. 72, 311–408.

Associate editor: James Van Orman